

# 聚醚醚酮与不同硬质涂层配副的摩擦学行为对比

周小卉<sup>1,2</sup>, 孙丽丽<sup>1</sup>, 蒋先春<sup>1</sup>, 崔丽<sup>1</sup>,  
汪爱英<sup>1,3</sup>, 崔平<sup>2,3</sup>, 柯培玲<sup>1,3</sup>

(1.中国科学院宁波材料技术与工程研究所 a.中国科学院海洋新材料与应用技术重点实验室 b.浙江省海洋材料与防护技术重点实验室, 浙江 宁波 315201; 2.上海科技大学 物质科学与技术学院, 上海 201210; 3.中国科学院大学, 北京 100049)

**摘要:** **目的** 对比聚醚醚酮 (PEEK) 与不锈钢、CrN 涂层、Cr/GLC 多层涂层 3 种配副的大气环境摩擦学行为。**方法** 采用多靶磁控溅射镀膜技术在 17-4PH 不锈钢基底表面制备 CrN 涂层和 Cr/GLC 多层涂层。采用摩擦磨损试验机和三维轮廓仪对配副摩擦因数和磨损率进行测试, 采用扫描电镜、拉曼光谱仪和显微红外光谱仪等方法, 表征不同配副摩擦前后的表面物理化学状态, 剖析涂层与 PEEK 配副的磨损机理。**结果** CrN 涂层和 Cr/GLC 多层涂层均显著提高了不锈钢基底的摩擦性能, 相较于 PEEK 与 17-4PH 不锈钢配副, CrN 涂层和 Cr/GLC 多层涂层的摩擦系数都显著降低。此外, 涂层的磨损率分别降低了 93.1%、97.4%; 对应 PEEK 配副的磨损体积也分别降低了 35.1% 和 65.8%。在 3 种配副条件下, PEEK 摩擦后均发生了芳香环的开放、取代、交联, 以及不同程度的结晶度损失, 结晶度的顺序为未磨 PEEK>PEEK-Cr/GLC>PEEK-CrN>PEEK-17-4。**结论** CrN 涂层的硬度、粗糙度较高, 且缺少润滑, 黏着磨损更显著, PEEK 材料发生了大量转移, 转移材料在减轻 PEEK 磨损的同时也阻止了结晶度的降低。PEEK 与 Cr/GLC 多层涂层配副表现出最佳的耐磨损性能, 主要归因于摩擦时 PEEK 结晶度的维持及 GLC 中富石墨相赋予涂层的低剪切润滑作用。

**关键词:** 硬质涂层; 非晶碳; 石墨相; 聚醚醚酮; 摩擦; 结晶度

中图分类号: TG115.5+8 文献标识码: A 文章编号: 1001-3660(2023)06-246-10

DOI: 10.16490/j.cnki.issn.1001-3660.2023.06.021

## Comparison of Tribological Behavior of Polyetheretherketone Matched with Different Hard Coatings

ZHOU Xiao-hui<sup>1,2</sup>, SUN Li-li<sup>1</sup>, JIANG Xian-chun<sup>1</sup>, CUI Li<sup>1</sup>, WANG Ai-ying<sup>1,3</sup>, CUI Ping<sup>2,3</sup>, KE Pei-ling<sup>1,3</sup>

(1. a. Key Laboratory of Marine Materials and Related Technologies, b. Zhejiang Key Laboratory of Marine Materials and Protective Technologies, Ningbo Institute of Materials Technology and Engineering, Chinese Academy of Sciences, Ningbo 315201, China; 2. School of Physical Science and Technology, Shanghai Tech University, Shanghai 201210, China; 3. University of Chinese Academy of Sciences, Beijing 100049, China)

收稿日期: 2022-05-06; 修订日期: 2022-10-26

Received: 2022-05-06; Revised: 2022-10-26

基金项目: 中国科学院 A 类战略性先导科技专项 (XDA22010303); 中科院创新团队 (292020000008); 浙江省自然科学基金 (LQ20E020004); 宁波市科技创新 2025 重大专项 (2022Z054)

Fund: A-Class Pilot of the Chinese Academy of Sciences (XDA22010303); CAS Interdisciplinary Innovation Team (292020000008); Zhejiang Provincial Natural Science Foundation of China (LQ20E020004); Ningbo Science and Technology 2025 Innovation Project (2022Z054)

作者简介: 周小卉 (1998—), 女, 硕士生, 主要研究方向为严苛环境防护涂层技术。

Biography: ZHOU Xiao-hui (1998-), Female, Postgraduate, Research focus: coating technology for harsh environment protection.

通讯作者: 柯培玲 (1979—), 女, 博士, 研究员, 主要研究方向为减摩耐磨防护涂层。

Corresponding author: KE Pei-ling (1979-), Female, Doctor, Professor, Research focus: antifriction and wear resistant protective coating.

引文格式: 周小卉, 孙丽丽, 蒋先春, 等. 聚醚醚酮与不同硬质涂层配副的摩擦学行为对比[J]. 表面技术, 2023, 52(6): 246-255.

ZHOU Xiao-hui, SUN Li-li, JIANG Xian-chun, et al. Comparison of Tribological Behavior of Polyetheretherketone Matched with Different Hard Coatings[J]. Surface Technology, 2023, 52(6): 246-255.

**ABSTRACT:** The surface coating technology can improve the friction and wear behavior of the substrate while maintaining its excellent mechanical properties. CrN coating as the representative of hard coating materials with high hardness can effectively resist impact and abrasive wear, and is often used in mechanical bearing shaft, piston pin and other friction protection. Diamond like carbon (DLC) coating is a kind of metastable material formed by the  $sp^2$  and  $sp^3$  hybrid of carbon, which has high hardness, wear resistance, chemical inertia and other properties. In particular, graphite-like carbon (GLC) coating, which is dominated by graphite-phase  $sp^2$  hybrid bond content, shows better adaptability to multiple environments. In order to carry out the technical optimization of polyetheretherketone (PEEK) matching materials, and solve the problem of easy wear of PEEK material of PEEK-stainless steel friction system, the work aims to compare and investigate the tribological behavior of PEEK matched with stainless steel, CrN and Cr/GLC coatings.

CrN and Cr/GLC multi-layer coatings were prepared on 17-4PH stainless steel substrate (the size was  $\phi 17$  mm  $\times$  3 mm) by multi-target magnetron sputtering deposition system. The coating thickness was about 1.8  $\mu$ m and 2  $\mu$ m, respectively. The friction testing machine was used to test the relationship between COF and time. The matching pair was PEEK ball with a diameter of 6 mm. The coating wear rate was calculated by 3D profilometer. The wear volume of three kinds of matching PEEK balls was calculated according to the volume of the crown. The physical and chemical states of the coatings were characterized by SEM, Raman and FTIR, etc., and the wear mechanism between the coatings and PEEK was analyzed.

The results showed that both CrN and Cr/GLC multi-layer coatings could improve the friction properties when they were matched with PEEK. Compared with stainless steel, the COF of CrN and Cr/GLC coatings reduced significantly. The wear rate of CrN coating and Cr/GLC coating decreased 93.1% and 97.4%. The wear volume for counterpart PEEK decreased by 35.1% and 65.8%, respectively. The aromatic ring opening, replacement, cross-linking, and loss of crystallinity occurred in PEEK surface during sliding process, and the crystallinity was as follows: unworn PEEK > PEEK grinding with Cr/GLC > PEEK grinding with CrN > PEEK grinding with 17-4.

When PEEK was against 17-4 PH stainless steel, the micro-convex of the substrate spalled and hard particles were formed, resulting in abrasive wear. Part of the PEEK transferred to the substrate surface and another part of the formation of wear debris piled up on the edge of the grinding crack, caused by wear sharp PEEK surface crystallinity slash and mechanics performance, eventually leading to the decrease of the material abrasion resistance. When PEEK is matched with CrN coating, because the CrN coating surface is rough and lack of lubrication, it can plough the PEEK surface, which makes the adhesive wear more significant. A large amount of PEEK material transfer occurs and the transfer material can reduce PEEK wear and prevent the decrease of crystallinity. When PEEK is matched with Cr/GLC coating, it is attributed to the good crystallinity stability of PEEK and excellent lubrication of graphite structure in Cr/GLC multi-layer coating.

**KEY WORDS:** hard coating; amorphous carbon; graphite structure; polyetheretherketone; wear; crystallinity

聚醚醚酮 (Polyetheretherketone, PEEK) 是一种典型的高性能半结晶聚合物, 具有极高的耐热性, 良好的化学惰性和韧性, 优异的耐磨损性能<sup>[1]</sup>, 近年来广泛应用于医疗、能源等领域。尤其是聚醚醚酮具有良好的减磨润滑作用, 常用于不锈钢摩擦副系统中, 以获得低摩擦因数<sup>[2]</sup>。研究者普遍认为, PEEK 提高润滑性能的重要作用之一是在钢表面形成了转移膜<sup>[3-4]</sup>, 并常作为固体润滑剂, 用于不锈钢-不锈钢摩擦体系中<sup>[5]</sup>。由于润滑转移膜的形成常伴随着聚合物材料的磨损, 这会导致高密封精密部件的密封性失效, 严重影响设备的长寿命可靠运行, 因此亟须开展配副材料技术优化, 解决 PEEK-不锈钢摩擦体系 PEEK 材料易磨损的问题。

表面涂层技术在保持基体优异的力学性能的同时, 可改善其摩擦磨损行为。以 CrN 涂层为代表的硬质涂层材料的硬度 (可达 19 GPa) 较高, 可有效

抵抗冲击和磨粒磨损, 常被应用于机械轴承、活塞销等摩擦防护领域<sup>[6]</sup>。Li 等<sup>[7]</sup>研究发现, CrN 涂层在甘油、大豆油等多种润滑油下具有强适应性, 能够有效提高不锈钢的摩擦性能。类金刚石 (Diamond like carbon, DLC) 涂层是一类由碳的  $sp^2$  和  $sp^3$  杂化形成的一种亚稳态材料, 兼具高硬度、耐磨、化学惰性等性能。尤其是以石墨相  $sp^2$  杂化键含量占主导的类石墨涂层 (Graphite like carbon, GLC), 它呈现出更优异的适应多种环境的摩擦性能。Stallard 等<sup>[8]</sup>研究发现, GLC 涂层在空气、油、水 3 种环境中均表现出较低的摩擦因数和磨损率。

目前, 研究者已经开展了 CrN 涂层和 GLC 涂层与塑料配副的摩擦性能研究。冶艳等<sup>[9]</sup>对比了 CrN 涂层与聚酰胺 66 (PA66) 和丙烯腈-丁二烯-苯乙烯共聚物 (ABS) 配副的磨损行为, 发现 CrN 涂层提高了钢-塑料配副的摩擦性能, 并将这种性能的提升归结

为涂层的高硬度和低表面粗糙度。Guan 等<sup>[10]</sup>比较了聚醚醚酮 (PEEK)、聚酰亚胺 (PI) 等塑料与 GLC 涂层配副的摩擦性能, 发现 PEEK 与 GLC 涂层呈现出相对最佳的对偶配副。CrN 涂层、GLC 涂层展现出稳定的减磨作用, 使其成为 PEEK 摩擦防护的理想之选。CrN 涂层的耐磨性能通常取决于其本身的高硬度, GLC 涂层的耐磨性与摩擦界面处的转移膜有关, 不同涂层与 PEEK 对磨时的界面演变特性将决定 PEEK-不锈钢摩擦体系的摩擦特性。目前, 针对 PEEK 材料与 CrN、GLC 涂层之间的摩擦学行为的研究鲜见报道, 对于金属、氮化物及具有润滑性能的 GLC, 其表面键态结构对 PEEK 转移膜的影响规律尚不明确, 适合 PEEK 材料的摩擦配副涂层仍在探索阶段。

磁控溅射技术是制备 CrN、GLC 涂层的重要方法之一, 利用该技术可以制备出低内应力的 GLC 涂层<sup>[11]</sup>。通过高功率脉冲磁控溅射技术 (High Power Impulse Magnetron Sputtering, HIPIMS) 可实现对 CrN 涂层组分和结构的调控, 提高涂层的致密性和均匀性<sup>[12]</sup>。基于此, 笔者采用多靶磁控溅射镀膜技术分别制备 CrN 涂层和 Cr/GLC 多层涂层<sup>[13]</sup>, 对比研究 17-4PH 不锈钢基底、CrN 涂层、Cr/GLC 多层涂层与 PEEK 配副的摩擦学行为, 并结合摩擦表面物理化学状态分析, 对其机理进行解释, 相关结果可为 PEEK-对偶配副设计提供实验与理论基础。

## 1 实验

### 1.1 涂层制备

采用多靶磁控溅射镀膜技术, 在尺寸为  $\phi 17 \text{ mm} \times 3 \text{ mm}$  的 17-4PH 不锈钢基底上分别沉积 CrN 涂层和 Cr/GLC 多层涂层。在镀膜前, 将基底分别在丙酮、无水乙醇中清洗, 每次清洗 10 min; 然后用导电胶将基底均匀贴附在样品台上, 并放入真空腔室作为本底, 真空抽至  $5.3 \times 10^{-3} \text{ Pa}$  时, 采用直流电源刻蚀基底, 氩气的流量为 35 mL/min, 随后开始制备涂层。

Cr/GLC 多层涂层制备过程: 首先在表面沉积过渡层 Cr 层和 CrN 层, 将功率控制在 1.8 kW, 偏压为 100 V, 共沉积 8 min, 过渡层的厚度约为 150 nm; 然后交替沉积 GLC 层和 Cr 层, 周期为 14 个, GLC 层的偏压为 200 V, 功率约为 2.0 kW, 沉积时间为 22 min, Cr 层的偏压为 100 V, 功率为 1.6 kW, 沉积时间为 4 min, 每层厚度约为 95 nm; 最后, 沉积顶层 GLC, 沉积时间为 50 min, 顶层厚度约为 230 nm。涂层的总厚度约为 1.8  $\mu\text{m}$ 。

采用高功率脉冲磁控溅射技术 (HiPIMS) 制备 CrN 涂层, 将功率控制在 3.0 kW, 偏压为 200 V, 保持腔体压力为 0.5 Pa。首先在基底表面沉积过渡层 Cr 层, 沉积时间为 10 min, 过渡层厚度约为 250 nm。然后在表面沉积 CrN 层, 沉积时间为 120 min, 厚度约为 1.8  $\mu\text{m}$ 。涂层总厚度约为 2  $\mu\text{m}$ 。Cr/GLC 多层涂层和 CrN 涂层具体的沉积参数如表 1 所示。

### 1.2 性能测试和微观结构表征

为了对比 PEEK 与不锈钢、CrN 涂层、Cr/GLC 多层涂层配副的摩擦学性能, 采用 Rtec 摩擦磨损试验机测试配副摩擦因数随时间的变化情况。摩擦测试参数: 载荷为 5 N, 频率为 2 Hz, 摩擦长度为 5 mm, 摩擦时间为 60 min。对磨配副为直径 6 mm 的 PEEK 球 (亿欣球业), 其拉伸强度约为 90 MPa, 弯曲强度约为 150 MPa, 密度约为 1.3 g/cm<sup>3</sup>。采用三维光学轮廓仪测量并计算磨损率, 见式 (1)<sup>[14]</sup>。

$$W = \frac{S \times l}{N \times L} \quad (1)$$

式中:  $S$  为磨痕截面积;  $l$  为磨痕长度;  $N$  为施加载荷;  $L$  为摩擦总距离。

将磨斑半径近似为被切削的球冠体积半径, 由此得出 PEEK 球的磨损体积, 见式 (2)。

$$V = \frac{\pi}{3} (R - \sqrt{R^2 - r^2})^2 (2R + \sqrt{R^2 + r^2}) \quad (2)$$

式中:  $R$  为 PEEK 球半径;  $r$  为磨斑半径。

表 1 Cr/GLC 多层涂层与 CrN 涂层的沉积参数

Tab.1 Deposition parameters of Cr/GLC multi-layer coating and CrN coating

Coating	Procedure	Power/kW	N <sub>2</sub> flow/(mL·min <sup>-1</sup> )	Ar flow/(mL·min <sup>-1</sup> )	Bias voltage/V	Time/min
	Etching			35	-200	40
	Cr transition layer	1.8		55	-100	4
	CrN transition layer	1.8	20	55	-100	4
Cr/GLC	GLC layer	2.0		55	-200	22
	Cr layer	1.6		55	-100	4
	GLC top layer	2.0		55	-200	50
CrN	Cr transition layer	3.0		50	-200	10
	CrN layer	3.0	30	Keep the chamber pressure at 0.5 Pa	-200	120

为了剖析 3 种配副的磨损机理, 采用场发射扫描电镜热场 Quanta 250 和场发射扫描电镜冷场 S4800 观察涂层的截面、表面形貌; 采用原子力显微镜 (AFM, 3100v, Veeco, USA) 测量表面粗糙度, 扫描频率为 2 Hz; 采用高功率转靶多晶 X 射线衍射仪 90WEI (XRD) 表征 CrN 涂层结构; 采用纳米压痕仪 (G200, MTS, USA) 测试涂层的硬度 ( $H$ ) 和弹性模量 ( $E$ ), 测试时取涂层表面平整位置, 测试 8 个点, 并取其平均值; 采用共聚焦显微拉曼光谱仪 (RENISHAW) 观察涂层摩擦前后微结构的变化 (激发光为波长 532 nm 的可见光) 和 PEEK 磨斑结构 (激发光为波长 785 nm 的可见光); 通过显微红外光谱仪 (Micro-FTIR) 对 PEEK 表面摩擦前后的结构变化进行表征。

## 2 结果及分析

### 2.1 涂层结构及力学性能

沉积态 CrN 涂层的 SEM 截面形貌如图 1a 所示, 涂层呈柱状晶结构, 厚度约为 2  $\mu\text{m}$ 。通过 XRD 谱图 (如图 1b 所示) 可以看出, CrN 涂层存在 (111)、(200)、(110)、(220)、(211) 衍射峰, 其中 (220) 晶面衍射峰的强度最大, 呈现明显的择优取向。

沉积态 Cr/GLC 多层涂层的截面 SEM 图如图 1c 所示, 暗区为 GLC 层, 亮区为 Cr 层, Cr 层呈现柱状晶结构, GLC 层为典型的非晶结构, 二者交替排列, 涂层的厚度约为 1.8  $\mu\text{m}$ 。类金刚石涂层在波长为 532 nm 的可见光激发光源下的拉曼光谱通常在约 1500  $\text{cm}^{-1}$  附近出现一个不对称的宽峰, 通过高斯或者洛伦兹拟合可以得到 2 个分别位于 1360  $\text{cm}^{-1}$  的 D 峰和 1550  $\text{cm}^{-1}$  的 G 峰<sup>[15-16]</sup>。通过对拉曼光谱的拟合分析, 可以得到 G 峰与 D 峰的面积之比  $I_D/I_G$ 、G 峰峰位  $G_{\text{peak position}}$  及 G 峰半高宽  $G_{\text{FWHM}}$  等信息<sup>[17]</sup>。沉积态 Cr/GLC 多层涂层表面拉曼光谱如图 1d 所示, G 峰与 D 峰的面积之比  $I_D/I_G$  为 2.75, G 峰峰位为 1548.58  $\text{cm}^{-1}$ , G 峰半高宽  $G_{\text{FWHM}}$  为 182.97  $\text{cm}^{-1}$ 。

通过纳米压痕测试, 得到 17-4 PH 不锈钢、CrN 涂层和 Cr/GLC 多层涂层的硬度、弹性模量和  $H^3/E^2$ , 见表 2。可以看到, 2 种涂层都具有较高的硬度, 比基底硬度高 2~4 倍, 表明 2 种涂层的沉积都有效提升了不锈钢的耐磨性<sup>[18]</sup>。其中, CrN 涂层的硬度最高, 达到 19.56 GPa, 且其弹性模量最高, 达到 315.52 GPa, 表明其刚度大, 材料不易发生变形。 $H^3/E^2$  反映了材料能承受的接触屈服应力<sup>[19]</sup>。Cr/GLC 多层涂层的  $H^3/E^2$  最大, 达到 0.076, 表明其局部能量耗散小, 进一步说明 Cr/GLC 多层涂层的耐磨性较好。

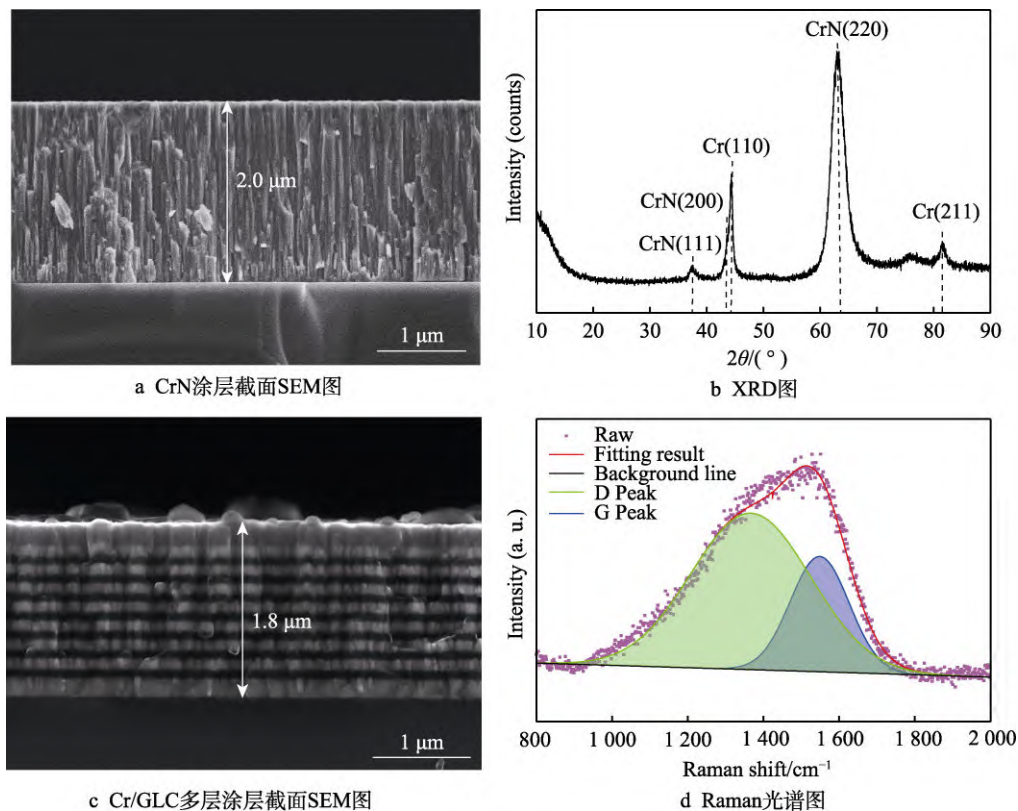


图 1 CrN 涂层与 Cr/GLC 多层涂层的结构信息

Fig.1 Structure information of CrN coating and Cr/GLC multi-layer coating: a) SEM cross-sectional image of CrN coating; b) XRD result; c) SEM cross-sectional image of Cr/GLC multi-layer coating; d) Raman spectrum

表2 17-4 PH 不锈钢、CrN 涂层、Cr/GLC 多层涂层的力学性能

Tab.2 Mechanical properties of the 17-4 PH stainless steel, CrN coating and Cr/GLC multi-layer coating

Samples	Hardness/GPa	Elasticity/GPa	$(H^3 \cdot E^{-2})/\text{GPa}$
17-4	5.15	227.20	0.002 6
CrN	19.56	315.52	0.075
Cr/GLC	14.75	205.99	0.076

17-4 PH 不锈钢基底与 2 种涂层的原子力显微图和平均粗糙度 (Average roughness,  $R_a$ ) 如图 2 所示。不锈钢基底较光滑,  $R_a$  仅为 4.95 nm。Cr/GLC 多层涂层的  $R_a$  为 9.85 nm, CrN 涂层的  $R_a$  高达 22.0 nm, 表明 CrN 涂层表面更粗糙。3 种材料的表面粗糙度不同, 可能会影响材料与 PEEK 配副摩擦时的磨损行为。

## 2.2 摩擦学性能

17-4PH 不锈钢、CrN 涂层、Cr/GLC 多层涂层与 PEEK 配副的摩擦系数随时间变化的情况如图 3 所示。在摩擦初期 (500 s 以内), 3 种配副的摩擦系数迅速上升, 然后随着摩擦时间的延长, 呈现不同的变

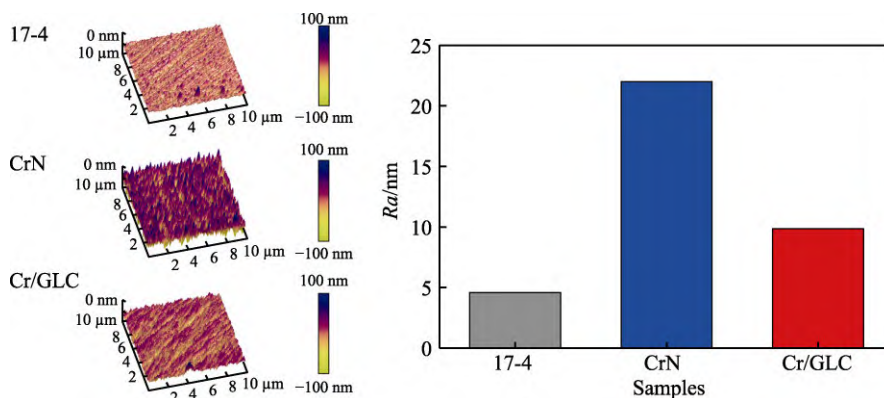


图2 17-4 PH 不锈钢、CrN 涂层、Cr/GLC 多层涂层的 AFM 图及  $R_a$

Fig.2 AFM diagram and  $R_a$  values of 17-4 PH stainless steel, CrN coating and Cr/GLC multilayer coating

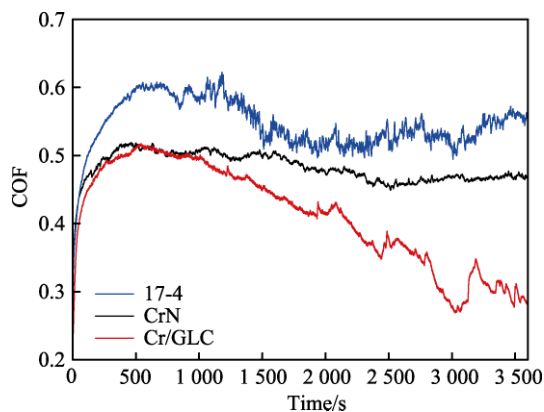


图3 PEEK 与 17-4 PH 不锈钢、CrN 涂层、Cr/GLC 多层涂层配副的摩擦系数-时间曲线

Fig.3 Friction coefficient-time curve of PEEK matched with 17-4 PH stainless steel, CrN coating and Cr/GLC multi-layer coating

化趋势。其中, PEEK 与 17-4 配副的摩擦系数从 0.6 左右逐渐下降, 在约 1 500 s 后达到 0.55 左右, 并保持稳定; PEEK 与 CrN 配副的摩擦系数从 0.52 左右缓慢下降, 在约 2 500 s 后达到 0.47 左右, 并保持稳定; PEEK 与 Cr/GLC 配副的摩擦系数从 0.5 左右持续降低, 在 1 h 时降至 0.3 左右。在 3 种配副中, PEEK 与 Cr/GLC 配副的摩擦系数在不同摩擦阶段均较低。

3 种配副磨损率对比如图 4 所示。17-4PH 不锈钢的磨损最严重, 其最大磨损深度为 2.20  $\mu\text{m}$ , 磨损率为  $1.51 \times 10^{-5} \text{ mm}^3/(\text{N} \cdot \text{m})$ 。CrN 涂层的最大磨损深度为 0.41  $\mu\text{m}$ , 磨损率为  $1.04 \times 10^{-6} \text{ mm}^3/(\text{N} \cdot \text{m})$ , 相较于 17-4PH 不锈钢, 其磨损率下降了约 93.1%。Cr/GLC 多层涂层的磨损最小, 最大磨损深度为 63.0 nm, 磨损率为  $3.91 \times 10^{-7} \text{ mm}^3/(\text{N} \cdot \text{m})$ , 相较于 17-4PH 不锈钢, 其磨损率下降了约 97.4%。

PEEK 与 17-4 配副的磨损体积为  $2.68 \times 10^{-3} \text{ mm}^3$ , PEEK 与 CrN 配副的磨损体积为  $1.74 \times 10^{-3} \text{ mm}^3$ , 相较于不锈钢基底配副, 其磨损体积下降了约 35.1%。PEEK 与 Cr/GLC 配副的磨损体积为  $9.16 \times 10^{-4} \text{ mm}^3$ , 相较于不锈钢基底配副, 磨损体积下降了约 65.8%。

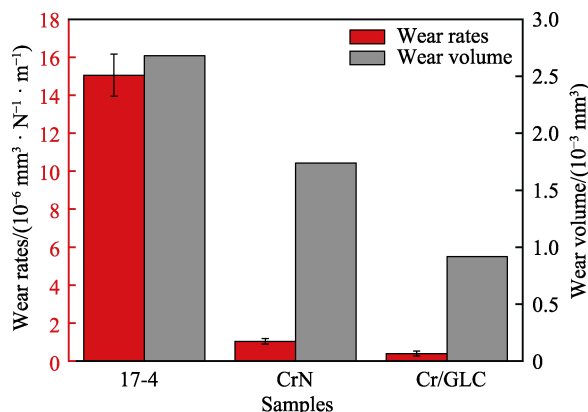


图4 17-4 PH 不锈钢、CrN 涂层、Cr/GLC 多层涂层磨损率与对磨 PEEK 磨损体积

Fig.4 Wear rate of 17-4 PH stainless steel, CrN coating and Cr/GLC multi-layer coating and corresponding wear volume of paired PEEK

由以上结果可以发现, CrN 涂层与 Cr/GLC 多层涂层均有效提高了 PEEK-不锈钢配副的摩擦学性能, 摩擦因数和磨损率显著降低。其中, PEEK-Cr/GLC 多层涂层配副的摩擦学性能最优。

### 2.3 磨痕及磨斑形貌

为了进一步剖析不同摩擦配副的摩擦行为, 考察了不同材料表面的磨痕、磨斑形貌, 以及对应的成分变化情况。从图 5a 可以发现, 磨痕表面存在明显的犁沟, 磨痕边缘存在磨屑堆积。进一步放大观察磨痕形貌发现, 在犁沟附近存在不均匀的 C、O 富集区, 且 2 种元素在聚集区重合, 表明 PEEK 材料发生了转移和磨损。在摩擦过程中, PEEK 材料一部分黏着在不锈钢表面, 一部分形成磨屑堆积在磨痕边缘。从图 5b 可知, 在磨斑处观察到明显的犁沟。在磨斑处, C、O 的不均匀分布明显, 说明 PEEK 球发生了严重的磨损。随着摩擦的进行, 磨屑堆积在犁沟凹陷处及磨斑周围, 在磨斑处有 Fe 元素黏附。说明 17-4PH 不锈钢基底也发生了严重的磨损, 摩擦副接触面产生的磨屑硬质颗粒造成基底和 PEEK 发生磨粒磨损。

与 17-4PH 不锈钢类似, CrN 涂层表面磨痕 (图 6a) 与对磨 PEEK 磨斑 (图 6b) 有较深的犁沟, 且磨痕边缘有磨屑堆积, 磨痕和磨斑内有大量的 C、O 富集区, 来自涂层的 Cr 元素黏附在 PEEK 磨斑处。此外, PEEK 转移材料在 CrN 涂层表面附着更多, 且沿摩擦方向呈平行分布。这是由于 PEEK 与 CrN 黏结

点的强度高于 2 种材料的强度, 剪切破坏主要发生在 PEEK 的表层内, 有时也发生在 CrN 表层内, 迁移到涂层上的黏着物使得软表面出现划痕, 所以擦伤主要发生在 PEEK 表面。相较于不锈钢基底, PEEK 与 CrN 涂层配副时的黏着磨损更显著。

Cr/GLC 多层涂层表面磨痕 (图 7a) 与 17-4PH 不锈钢和 CrN 涂层有着明显不同, 其磨痕较浅, 且无明显的 C、O 元素聚集。在磨斑处 (图 7b), Fe 元素面扫分布均匀, C、O 元素部分聚集, 但明显较 17-4 不锈钢磨痕和其配副 PEEK 磨斑均匀。说明 Cr/GLC 多层涂层的富石墨相结构表现出非常好的减磨润滑作用, 减轻了 PEEK 材料的磨损。

### 2.4 摩擦前后涂层与 PEEK 表面微结构

在摩擦前后, 17-4PH 不锈钢、CrN 涂层、Cr/GLC 多层涂层拉曼光谱对比如图 8 所示。相较于摩擦前, 摩擦后 17-4PH 不锈钢的拉曼光谱出现了典型的非晶碳峰, 并且在 CrN 磨痕表面检测到 C—O—C 醚拉伸 (约  $1147\text{ cm}^{-1}$ ) 和苯环 C=C 振动 (约  $1596\text{ cm}^{-1}$ ) 特征峰, 证实摩擦后 17-4PH 不锈钢与 CrN 涂层均与 PEEK 发生了黏着磨损, 导致软质 PEEK 发生转移。对于 Cr/GLC 多层涂层, 拉曼光谱 G 峰与 D 峰的面积之比  $I_D/I_G$  由 2.75 变为 2.72, G 峰峰位由  $1548.58\text{ cm}^{-1}$  变为  $1548.23\text{ cm}^{-1}$ , G 峰半高宽  $G_{FWHM}$  由 182.97 变为 185.397, 说明碳键结构未发生明显变化, 但  $G_{FWHM}$  的增大表明涂层的结构无序度增大, 来源于 C 的键角和

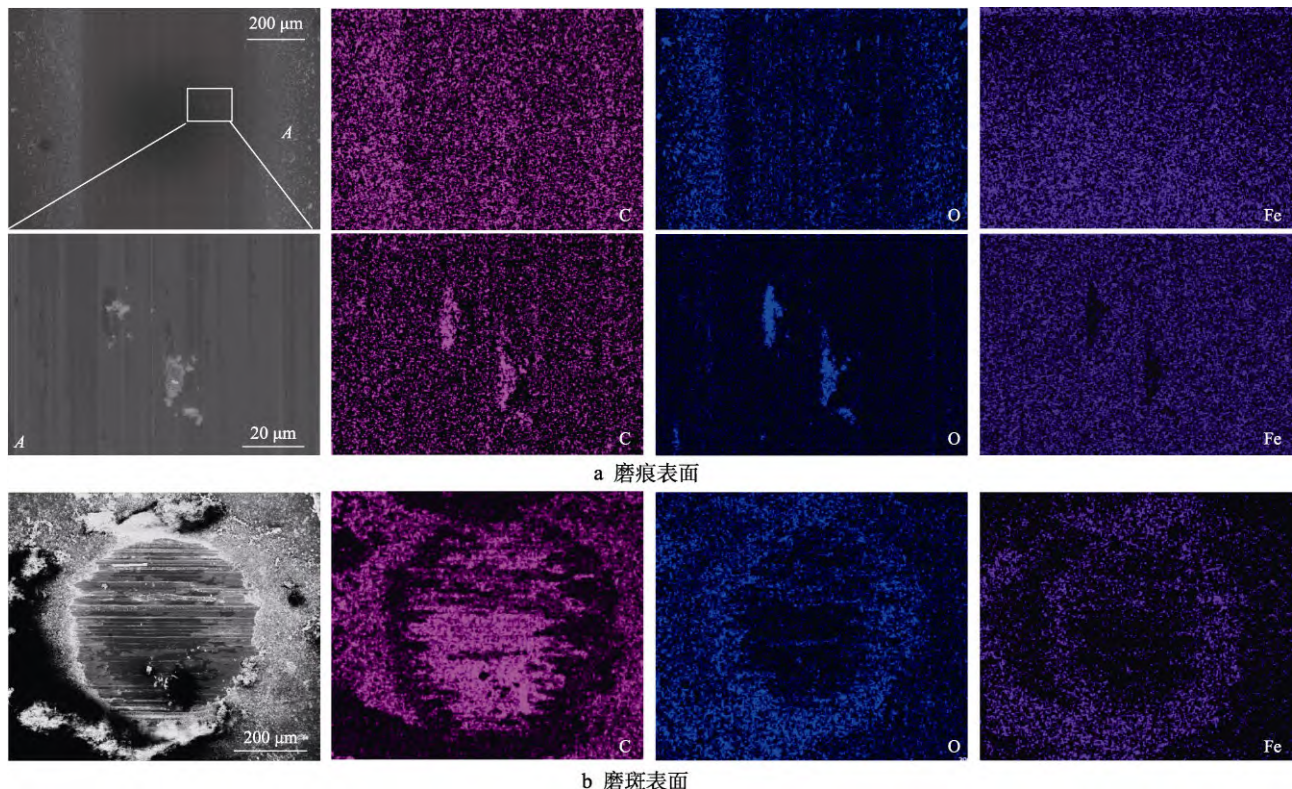


图 5 17-4PH 不锈钢磨痕与配副 PEEK 的 SEM 和面扫描元素分布

Fig.5 SEM and corresponding mapping image of 17-4PH stainless steel and paired PEEK wear track: a) wear track; b) wear scar

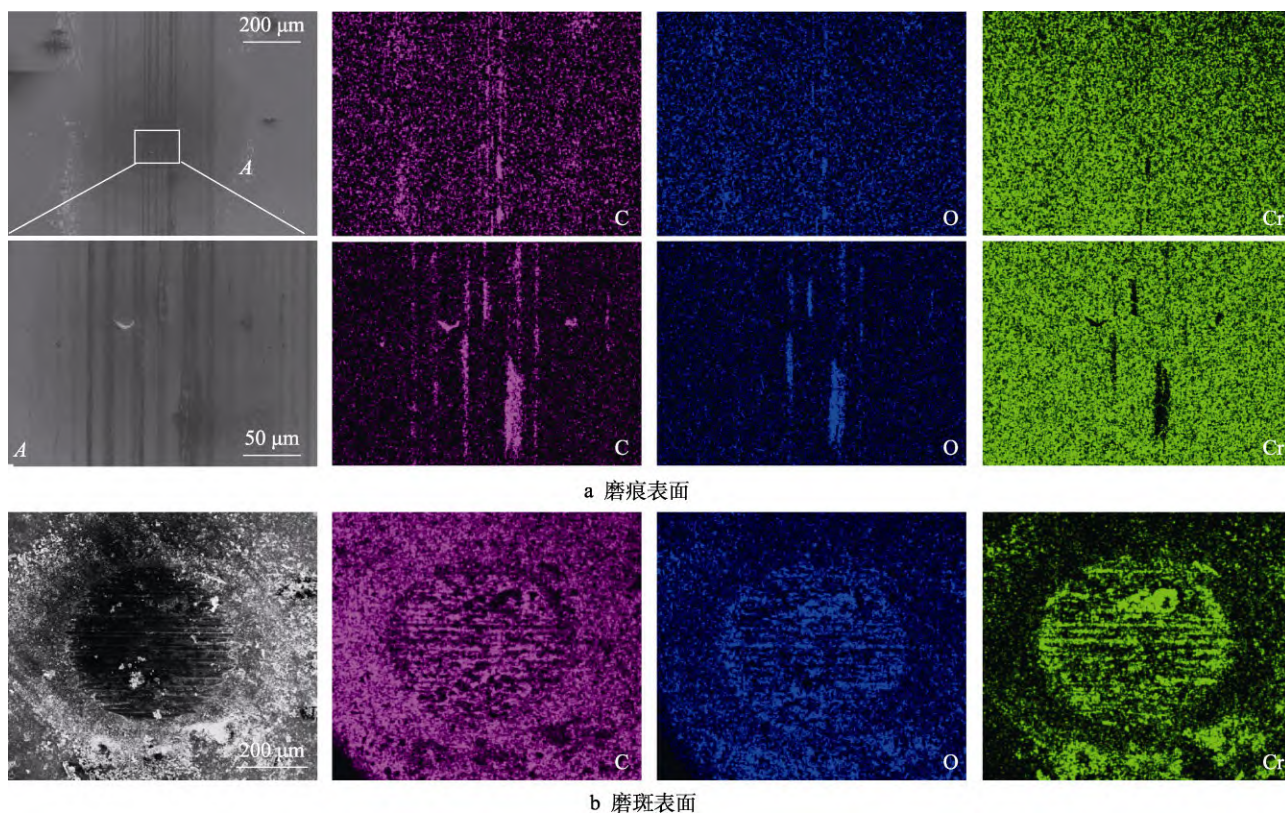


图 6 CrN 涂层磨痕与配副 PEEK 的 SEM 和面扫描元素分布  
Fig.6 SEM and corresponding mapping image of CrN coating and paired PEEK wear scar: a) wear track; b) wear scar

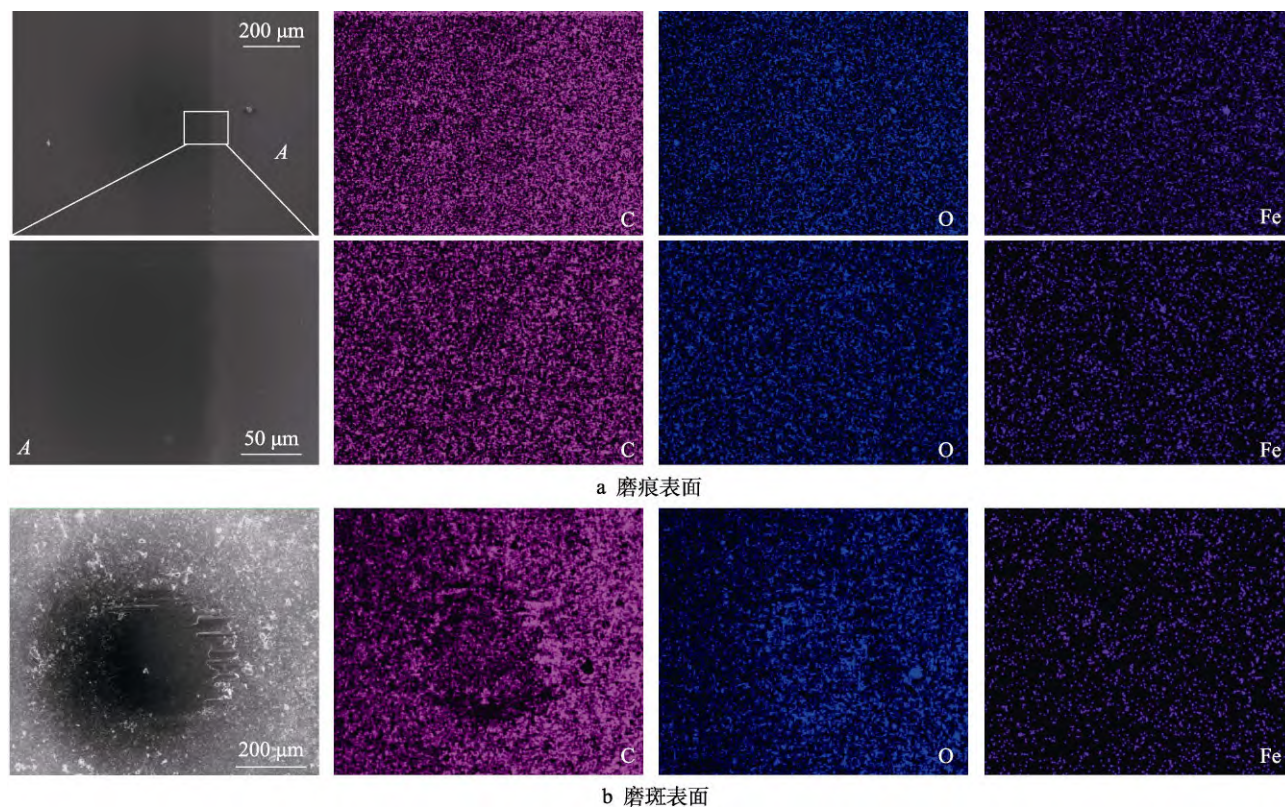


图 7 Cr/GLC 多层涂层磨痕与配副 PEEK 的 SEM 和面扫描元素分布  
Fig.7 SEM and corresponding mapping image of Cr/GLC multi-layer coating and and paired PEEK wear track: a) wear track; b) wear scar

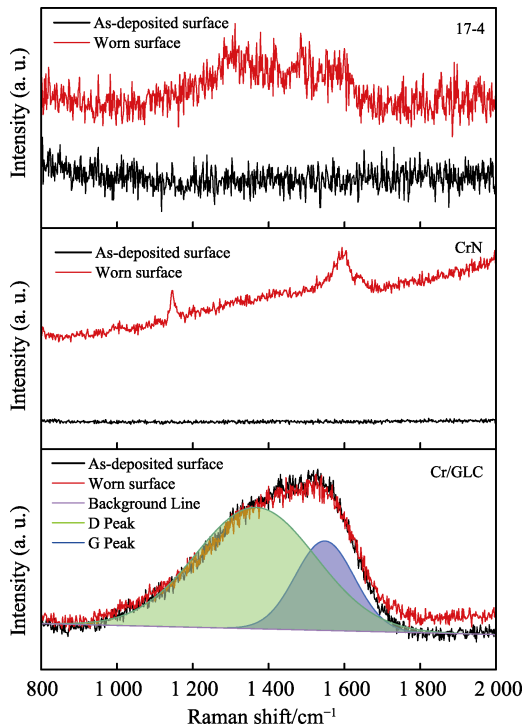


图 8 17-4PH 不锈钢、CrN 涂层、Cr/GLC 多层涂层摩擦前后拉曼光谱对比

Fig.8 Comparison of Raman spectra of 17-4PH stainless steel, CrN coating and Cr/GLC multi-layer coating before and after friction

键长的变化。这可能是由于摩擦接触面产生的低剪切力不足以使 GLC 表面形成更多的石墨化非晶结构<sup>[20-21]</sup>。

同时,对摩擦前后 PEEK 材料表面的微结构进行了拉曼光谱测试,结果如图 9 所示。在波数约为 807、1 147、1 596、1 646 cm<sup>-1</sup> 处的峰分别代表苯基环 C—H 拉伸振动、C—O—C 乙醚拉伸和弯曲、苯环 C=C 振动、C=O 拉伸振动<sup>[22-23]</sup>。PEEK 材料的  $I_{807}/I_{1596}$  与  $I_{1146}/I_{1596}$  峰高比值的变化反映了苯环键的氧化及乙醚键的交联断裂,  $I_{1147}/I_{1596}$  在一定程度上反映了 PEEK 材料结晶度的变化情况<sup>[24]</sup>。PEEK 摩擦后,

$I_{1147}/I_{1596}$ 、 $I_{807}/I_{1596}$  降低,  $I_{1646}/I_{1596}$  升高,说明 PEEK 发生了芳香环的开放、取代、交联及结晶度的丧失。

为了进一步验证 PEEK 结晶度的变化程度,通过傅里叶红外光谱图进行结晶度指数 ( $C_1$ ) 定量分析,如图 10 所示。在波数约为 1 650 cm<sup>-1</sup> 处的峰代表碳基的拉伸振动,1 305 cm<sup>-1</sup> 处为酮弯曲运动,926 cm<sup>-1</sup> 处为二苯醚的振动,1 185 cm<sup>-1</sup> 和 1 277 cm<sup>-1</sup> 为醚和二苯醚的吸收特征峰<sup>[25-26]</sup>。结晶度指数 ( $C_1$ ) 的定义见式 (3) (ASTM F 2778-09)。

$$C_1 = \frac{H_A}{H_B} \quad (3)$$

式中:  $H_A$  为 1 305 cm<sup>-1</sup> 左右的峰高;  $H_B$  为 1 280 cm<sup>-1</sup> 左右的峰高。

与 17-4PH 不锈钢、Cr 涂层、Cr/GLC 多层涂层配副,摩擦前后 PEEK 的结晶度指数如图 10b 所示,可以发现结晶度的顺序为未磨 PEEK>PEEK-Cr/GLC>PEEK-CrN>PEEK-17-4。对于聚合物材料,其高结晶度比低结晶度显示出更高的耐磨性,可通过结晶度定量分析聚合物材料的摩擦磨损程度<sup>[27-28]</sup>。PEEK 与 17-4PH 不锈钢基底配副时,其磨损剧烈,聚合物表面的结晶度明显降低,而结晶度的下降导致材料力学性能下降,进一步加剧磨损。PEEK 与 CrN 涂层配副时,摩擦后产生了大量材料转移,转移材料在减轻 PEEK 磨损的同时,也阻止了表面层结晶度的降低。PEEK 与 Cr/GLC 涂层配副时,由于 GLC 涂层为富石墨相结构,在摩擦过程中形成了低剪切力,能更好地维持 PEEK 的结晶度,保持其耐磨性。

## 2.5 磨损机理

通过分析配副摩擦前后的表面形貌及结构,提出 PEEK 与 17-4PH 不锈钢、CrN 涂层和 Cr/GLC 多层涂层配副的摩擦机理,如图 11 所示。PEEK 与 17-4PH 不锈钢基底配副摩擦时,基底微凸体剥落,形成硬质颗粒,造成磨粒磨损,对磨 PEEK 的一部分转移到基

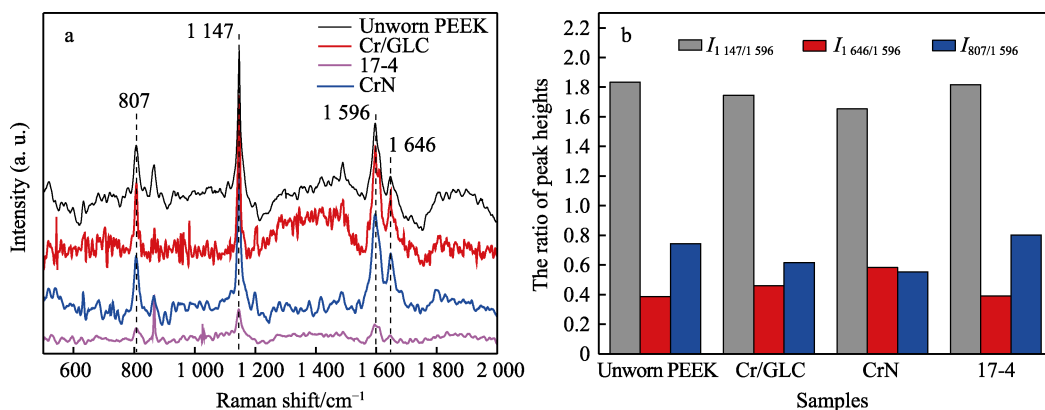


图 9 PEEK 与 17-4PH 不锈钢、CrN 涂层、Cr/GLC 多层涂层配副摩擦后,拉曼光谱 (a) 及各峰比值 (b)

Fig.9 Raman spectra (a) and peak ratio (b) of PEEK matched with 17-4PH stainless steel, CrN coating and Cr/GLC multi-layer coating after friction



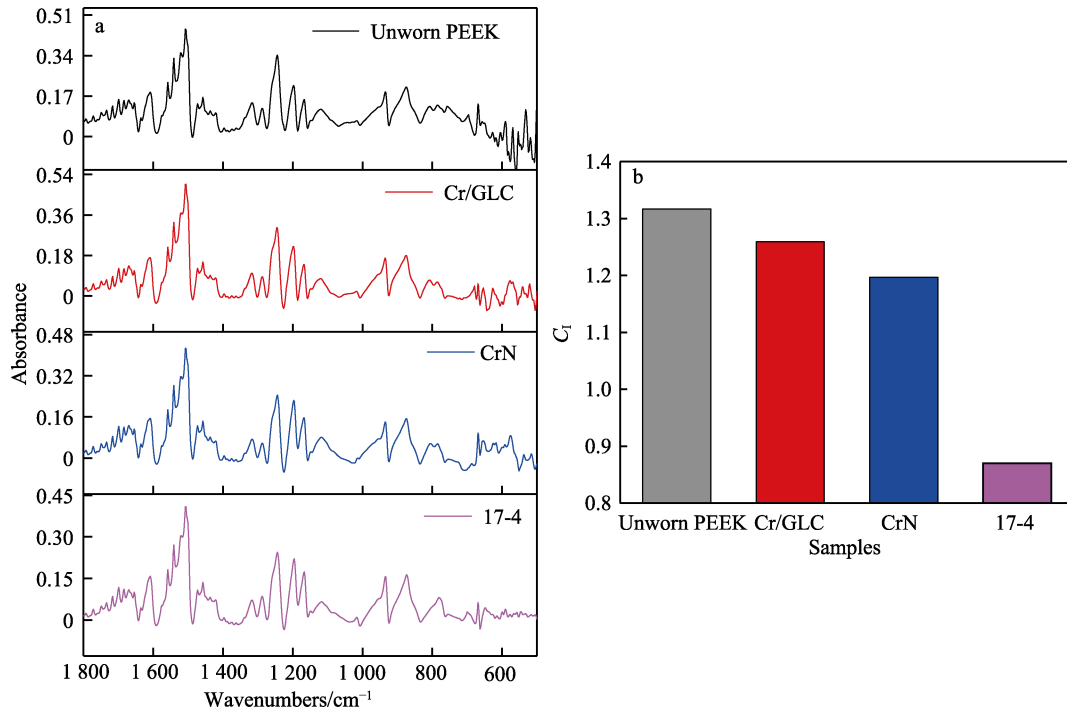


图 10 PEEK 与 17-4PH 不锈钢、CrN 涂层、Cr/GLC 多层涂层配副摩擦后红外光谱 (a) 及结晶度指数 (b)  
 Fig.10 Infrared spectrum (a) and crystallinity index (b) of PEEK matched with 17-4PH stainless steel, CrN coating and Cr/GLC multi-layer coating after friction

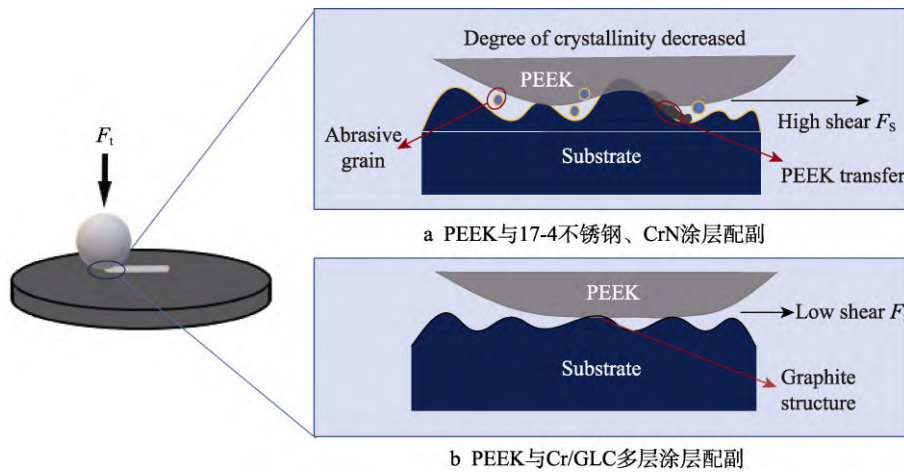


图 11 PEEK 与 17-4PH 不锈钢、CrN 涂层和 Cr/GLC 多层涂层配副摩擦机理  
 Fig.11 Friction mechanism of PEEK matched with 17-4PH stainless steel and CrN coating and Cr/GLC multi-layer coating: a) PEEK matched with 17-4PH stainless steel and CrN coating; b) PEEK matched with Cr/GLC multi-layer coating

底表面,另一部分形成磨屑,堆积在磨痕边缘。由于磨损剧烈,造成 PEEK 表面的结晶度大幅降低,力学性能下降,最终导致材料的耐磨性下降。PEEK 与 CrN 涂层配副的摩擦机理与 17-4PH 不锈钢类似。由于 CrN 涂层表面较粗糙,且缺少润滑,使得黏着磨损更显著<sup>[29]</sup>, PEEK 材料发生了大量转移,转移材料在减轻 PEEK 磨损的同时,也阻止了结晶度的降低。PEEK 与 Cr/GLC 涂层配副时,由于涂层为富石墨相结构,在摩擦过程中形成了低剪切力,能更好地维持 PEEK 结晶度,保持其耐磨性。

### 3 结论

1) 采用多靶磁控溅射镀膜技术,在 17-4PH 不锈钢基底分别制备了 CrN 涂层和 Cr/GLC 多层涂层,有效地提高了 PEEK-不锈钢配副的摩擦性能,其摩擦因数、涂层磨损率和 PEEK 球磨损体积均显著下降。其中,PEEK-Cr/GLC 多层涂层配副的摩擦学性能最优,涂层磨损率下降了 97.4%,PEEK 磨损体积下降了 65.8%。

2) 在干摩擦条件下, PEEK 摩擦后发生了芳香环的开放、取代、交联及结晶度的丧失。PEEK 与 17-4PH 不锈钢基底配副摩擦时, 基底微凸体剥落, 形成了硬质颗粒, 造成磨粒磨损。PEEK 与 CrN 涂层配副时, 由于 CrN 涂层表面较粗糙, 且缺少润滑, 对 PEEK 表面有犁削作用, 使得黏着磨损更显著, PEEK 材料发生大量转移。PEEK 与 Cr/GLC 涂层配副时, 由于涂层为富石墨相结构, 在摩擦过程中形成了低剪切力, 能更好地维持 PEEK 结晶度, 保持其耐磨性。

#### 参考文献:

- [1] 付国太, 刘洪军, 张柏, 等. PEEK 的特性及应用[J]. 工程塑料应用, 2006, 34(10): 69-71.  
FU Guo-tai, LIU Hong-jun, ZHANG Bai, et al. Characteristics and Applications of PEEK[J]. Engineering Plastics Application, 2006, 34(10): 69-71.
- [2] CHE Qing-lun, LI Hao, ZHANG Li-gang, et al. Role of Carbon Nanotubes on Growth of a Nanostructured Double-Deck Tribofilm Yielding Excellent Self-Lubrication Performance[J]. Carbon, 2020, 161: 445-455.
- [3] YE J, KHARE H S, BURRIS D L. Transfer Film Evolution and Its Role in Promoting Ultra-Low Wear of a PTFE Nanocomposite[J]. Wear, 2013, 297(1/2): 1095-1102.
- [4] ZUO Zhen, YANG Yu-lin, QI Xiao-wen, et al. Analysis of the Chemical Composition of the PTFE Transfer Film Produced by Sliding Against Q235 Carbon Steel[J]. Wear, 2014, 320: 87-93.
- [5] LIN Le-yu, EMRICH S, KOPNARSKI M, et al. Lubrication Performance of a Polyetheretherketone (PEEK) and Polytetrafluoroethylene (PTFE) Blend within a Steel/Steel Tribosystem[J]. Wear, 2021, 484/485: 203997.
- [6] LUBAS J. Tribological Properties of CrN Coating under Lubrication Conditions[J]. Surface Review and Letters, 2012, 19(4): 1250042.
- [7] LI Yang, CAO Lei, QI Cai-xia, et al. Low Friction of CrN Coatings in Presence of Glycerol[J]. Applied Surface Science, 2020, 514: 145890.
- [8] STALLARD J, MERCS D, JARRATT M, et al. A Study of the Tribological Behaviour of Three Carbon-Based Coatings, Tested in Air, Water and Oil Environments at High Loads[J]. Surface and Coatings Technology, 2004, 177/178: 545-551.
- [9] 冶艳, 尚魁平, 鲍明东, 等. CrN 硬质镀层对磨热固性塑料的摩擦学行为研究[J]. 表面技术, 2012, 41(1): 27-29.  
YE Yan, SHANG Kui-ping, BAO Ming-dong, et al. Study on Tribological Behavior of CrN Hard Film Against Thermosetting Plastics[J]. Surface Technology, 2012, 41(1): 27-29.
- [10] GUAN Xiao-yan, WANG Li-ping. The Tribological Performances of Multilayer Graphite-Like Carbon (GLC) Coatings Sliding Against Polymers for Mechanical Seals in Water Environments[J]. Tribology Letters, 2012, 47(1): 67-78.
- [11] YANG S, TEER D G. Investigation of Sputtered Carbon and Carbon/Chromium Multi-Layered Coatings[J]. Surface and Coatings Technology, 2000, 131(1/2/3): 412-416.
- [12] WU Zhong-zhen, TIAN Xiu-bo, GONG Chun-zhi, et al. Micrograph and Structure of CrN Films Prepared by Plasma Immersion Ion Implantation and Deposition Using HPPMS Plasma Source[J]. Surface and Coatings Technology, 2013, 229: 210-216.
- [13] LIU Ying-rui, DU Hong, ZUO Xiao, et al. Cr/GLC Multi-layered Coating in Simulated Deep-Sea Environment: Corrosion Behavior and Growth Defect Evolution[J]. Corrosion Science, 2021, 188: 109528.
- [14] CHEN Jia, CAI W. Effect of Scratching Frequency on the Tribocorrosion Resistance of Al-Mn Amorphous Thin Films[J]. Wear, 2019, 426/427: 1457-1465.
- [15] FERRARI A C, ROBERTSON J. Raman Spectroscopy of Amorphous, Nanostructured, Diamond-Like Carbon, and Nanodiamond[J]. Philosophical Transactions of the Royal Society of London Series A: Mathematical, Physical and Engineering Sciences, 2004, 362: 2477-2512.
- [16] FERRARI A C, ROBERTSON J. Resonant Raman Spectroscopy of Disordered, Amorphous, and Diamondlike Carbon[J]. Physical Review B, 2001, 64(7): 075414.
- [17] CASIRAGHI C, FERRARI A C, ROBERTSON J. Raman Spectroscopy of Hydrogenated Amorphous Carbons[J]. Physical Review B, 2005, 72(8): 085401.
- [18] ZHANG Ying-peng, WANG Qun, CHEN Gang, et al. Mechanical, Tribological and Corrosion Physiognomies of CNT-Al Metal Matrix Composite (MMC) Coatings Deposited by Cold Gas Dynamic Spray (CGDS) Process[J]. Surface and Coatings Technology, 2020, 403: 126380.
- [19] 马铭, 任瑛, 侯晓多, 等. 磁控溅射制备 AlCrWTaTiNb 高熵合金薄膜低温等离子体氮化[J]. 大连理工大学学报, 2019, 59(1): 28-34.  
MA Ming, REN Ying, HOU Xiao-duo, et al. Low Temperature Plasmatic Nitriding of AlCrWTaTiNb High Entropy Alloy Film Synthesized by Magnetron Sputtering[J]. Journal of Dalian University of Technology, 2019, 59(1): 28-34.
- [20] FONTAINE J, DONNET C, GRILL A, et al. Tribochemistry between Hydrogen and Diamond-Like Carbon Films[J]. Surface and Coatings Technology, 2001, 146/147: 286-291.
- [21] DONNET C, LE MOGNE T, PONSONNET L, et al. The Respective Role of Oxygen and Water Vapor on the Tribology of Hydrogenated Diamond-Like Carbon Coatings[J]. Tribology Letters, 1998, 4(3): 259-265.
- [22] DOUMENG M, MAKHLOUF L, BERTHET F, et al. A Comparative Study of the Crystallinity of Polyetheretherketone by Using Density, DSC, XRD, and Raman Spectroscopy Techniques[J]. Polymer Testing, 2021, 93: 106878.

(下转第 360 页)

- Friction and Wear Characteristics of Agglomerated Diamond Abrasives and Lapping Performance of Fixed Agglomerated Diamond Pads[J]. *Wear*, 2021, 470-471: 203598.
- [24] WANG Zi-kun, NIU Feng-li, ZHU Yong-wei, et al. Comparison of Lapping Performance between Fixed Agglomerated Diamond Pad and Fixed Single Crystal Diamond Pad[J]. *Wear*, 2019, 432-433: 202963.
- [25] CHEN Jia-peng, ZHU Nan-nan, NIU Feng-li, et al. Influence of Agglomerated Diamond Abrasive Wear on Sapphire Material Removal Behavior[J]. *Diamond and Related Materials*, 2020, 108: 107965.
- [26] CHEN Jia-peng, SUN Tao, SU Jian-xiu, et al. A Novel Agglomerated Diamond Abrasive with Excellent Micro-Cutting and Self-Sharpening Capabilities in Fixed Abrasive Lapping Processes[J]. *Wear*, 2021, 464-465: 203531.
- [27] NIU Feng-li, WANG Ke-rong, SUN Tao, et al. Lapping Performance of Mixed-Size Agglomerated Diamond Abrasives in Fixed Abrasives Pads[J]. *Diamond and Related Materials*, 2021, 118: 108499.

责任编辑：刘世忠

(上接第 255 页)

- [23] PUHAN D, WONG J S S. Properties of Polyetheretherketone (PEEK) Transferred Materials in a PEEK-Steel Contact[J]. *Tribology International*, 2019, 135: 189-199.
- [24] DOUMENG M, FERRY F, DELBÉ K, et al. Evolution of Crystallinity of PEEK and Glass-Fibre Reinforced PEEK under Tribological Conditions Using Raman Spectroscopy[J]. *Wear*, 2019, 426/427: 1040-1046.
- [25] ZHAO Feng, LI Di-chen, JIN Zhong-min. Preliminary Investigation of Poly-Ether-Ether-Ketone Based on Fused Deposition Modeling for Medical Applications[J]. *Materials*, 2018, 11(2): 288.
- [26] AL-MUFTI S M S, ALI M M, RIZVI S J A. Synthesis and Structural Properties of Sulfonated Poly Ether Ether Ketone (SPEEK) and Poly Ether Ether Ketone (PEEK)[C]// AIP Conference Proceedings", "3rd International Conference on Condensed Matter and Applied Physics (ICC-2019), 2020: 020009
- [27] BRUCK A L, KANAGA KARUPPIAH K S, SUNDARARAJAN S, et al. Friction and Wear Behavior of Ultrahigh Molecular Weight Polyethylene as a Function of Crystallinity in the Presence of the Phospholipid Dipalmitoyl Phosphatidylcholine[J]. *Journal of Biomedical Materials Research Part B: Applied Biomaterials*, 2010, 93B(2): 351-358.
- [28] FAREED M I. Effect of Operating Conditions on the Tribological Performance of Polyether Ether Ketone (PEEK)[J]. *Advances in Polymer Technology*, 2018, 37(5): 1537-1543.
- [29] WANG A, ESSNER A, POLINENI V K, et al. Lubrication and Wear of Ultra-High Molecular Weight Polyethylene in Total Joint Replacements[J]. *Tribology International*, 1998, 31(1/2/3): 17-33.

责任编辑：彭颀

(上接第 284 页)

- [27] LI S, XU M M, ZHANG C Y, et al. Co-Doping Effect of Hf and Y on Improving Cyclic Oxidation Behavior of (Ni, Pt)Al Coating at 1 150 °C[J]. *Corrosion Science*, 2021, 178: 109093.
- [28] YAN Kai, GUO Hong-bo, GONG Sheng-kai. High-Temperature Oxidation Behavior of Minor Hf Doped NiAl Alloy in Dry and Humid Atmospheres[J]. *Corrosion Science*, 2013, 75: 337-344.
- [29] GUO Hong-bo, SUN Li-dong, LI He-fei, et al. High Temperature Oxidation Behavior of Hafnium Modified NiAl Bond Coat in EB-PVD Thermal Barrier Coating System[J]. *Thin Solid Films*, 2008, 516(16): 5732-5735.
- [30] SUN li dong, GUO hong bo, LI he fei, et al. Hf Modified NiAl Bond Coat for Thermal Barrier Coating Application[J]. *Materials Science Forum*, 2007, 546-549: 1777-1780.
- [31] PENG X, LI T, PAN W P. Oxidation of a La<sub>2</sub>O<sub>3</sub>-Modified Aluminide Coating[J]. *Scripta Materialia*, 2001, 44(7): 1033-1038.
- [32] YANG J C, SCHUMANN E, LEVIN I, et al. Electron Microscopy Studies of the High Temperature Oxidation Behavior of NiAl[J]. *MRS Online Proceedings Library*, 1996, 466(1): 197-202.
- [33] LIPKIN D M, SCHAFFER H, ADAR F, et al. Lateral Growth Kinetics of A-Alumina Accompanying the Formation of a Protective Scale on (111) NiAl during Oxidation at 1 100 °C [J]. *Applied Physics Letters*, 1997, 70(19): 2550-2552.

责任编辑：彭颀